

Complex Correspondence Principle

Carl M. Bender^{1,*}, Daniel W. Hook^{2,†}, Peter N. Meisinger^{1,‡} and Qing-hai Wang^{3,§}

¹*Department of Physics, Washington University, St. Louis, MO 63130, USA*

²*Theoretical Physics, Imperial College London, London SW7 2AZ, UK*

³*Department of Physics, National University of Singapore, Singapore 117542*

(Dated: December 10, 2009)

Quantum mechanics and classical mechanics are two very different theories, but the correspondence principle states that quantum particles behave classically in the limit of high quantum number. In recent years much research has been done on extending both quantum mechanics and classical mechanics into the complex domain. This letter shows that these complex extensions continue to exhibit a correspondence, and that this correspondence becomes more pronounced in the complex domain. The association between complex quantum mechanics and complex classical mechanics is subtle and demonstrating this relationship requires the use of asymptotics beyond all orders.

PACS numbers: 11.30.Er, 03.65.-w, 02.30.Fn, 05.40.Fb

The correspondence principle states that at high energy quantum mechanics resembles classical mechanics. In Fig. 1 we illustrate this resemblance for the harmonic oscillator Hamiltonian $H = p^2 + x^2$. We compare the quantum probability density $\rho_{\text{quantum}}(x) = |\psi_{16}(x)|^2$ for the 16th energy level $E_{16} = 33$ with the classical probability density $\rho_{\text{classical}}(x) = 1/s$, where s is the speed of the particle. In the classically allowed region, which is bounded by the classical turning points at $\pm\sqrt{33}$, $\rho_{\text{quantum}}(x)$ oscillates about $\rho_{\text{classical}}(x)$. The particle speed vanishes at the turning points, so $\rho_{\text{classical}}$ is singular. (This singularity is integrable and thus the classical probability is normalizable.) In the classically forbidden region $\rho_{\text{quantum}}(x)$ decays exponentially; in conventional classical mechanics the particle does not enter this region and its probability density is thought to vanish.

This paper generalizes quantum and classical probability into the complex domain. In complex classical mechanics we solve Hamilton's equations $\dot{x} = \frac{\partial H}{\partial p}$, $\dot{p} = -\frac{\partial H}{\partial x}$ for complex initial conditions and not just for initial conditions in the classically allowed region [1, 2, 3, 4, 5, 6, 7].

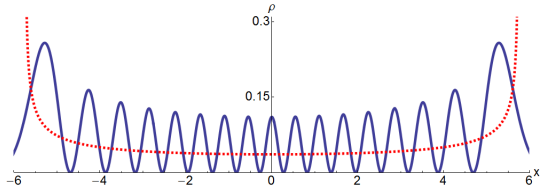


FIG. 1: Correspondence principle for the harmonic oscillator. The probability density $\rho(x) = |\psi_{16}(x)|^2$ for a quantum particle (solid curve) and the corresponding probability density for a classical particle of the same energy (dotted curve) are shown. In the parabolic potential well $\rho_{\text{quantum}}(x)$ is wavelike and oscillates closely about $\rho_{\text{classical}}(x)$. At the classical turning points, $\rho_{\text{classical}}(x)$ diverges. In the classically forbidden region the quantum particle density decays exponentially while the classical density is ordinarily assumed to vanish.

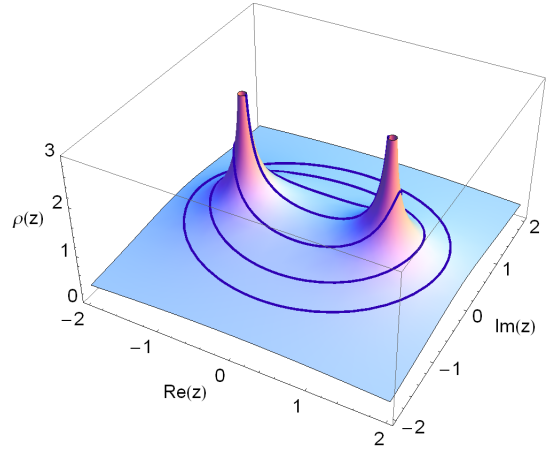


FIG. 2: Classical probability density at $z = x + iy$ in the complex plane for a particle of $E = 2$ in a harmonic potential. The probability density resembles a pup tent with infinitely high tent poles located at the turning points. The classical trajectories are nested ellipses, all of which have the same period $T = \pi$. These complex orbits are superposed on the tent canopy. The degenerate ellipse, whose foci are the turning points at $x = \pm\sqrt{E}$, is the conventional real solution. Classical particles repeatedly cross the real axis in the classically forbidden regions $|x| > \sqrt{E}$.

For the harmonic oscillator the classical orbits are nested ellipses with foci at the turning points. Using ρ_{quantum} in Fig. 1 as a guide, we require the probability of a classical particle being on more distant ellipses to decay exponentially, and we plot in Fig. 2 the relative probability density of finding the classical particle at the point $z = x + iy$.

Figure 2 shows that, contrary to the traditional view, the classical particle density in the classically forbidden region is actually nonzero, and that $\rho_{\text{classical}}$ resembles ρ_{quantum} in this region [8]. This figure emphasizes that the classical probability density extends beyond the real axis and into the complex plane, where $\rho_{\text{classical}}(x, y)$ falls

off as the reciprocal of the distance from the origin.

To establish the complex correspondence principle we must continue the quantum probability density into the complex plane to match the complex classical probability density in Fig. 2. To do so we must extend quantum mechanics into the complex domain [9]. A Hermitian Hamiltonian ($H = H^\dagger$) has real energy levels and unitary time evolution. However, the class of physically allowable Hamiltonians may be extended to include non-Hermitian Hamiltonians that possess an unbroken \mathcal{PT} (combined parity and time-reversal) symmetry [10, 11, 12, 13, 14, 15]. These complex Hamiltonians also have real spectra and generate unitary time evolution, and such Hamiltonians have recently been observed in the laboratory [16, 17, 18].

For \mathcal{PT} -symmetric Hamiltonians the potential satisfies $V^*(-z) = V(z)$. This allows us to derive a conservation law in the complex plane from the time-dependent Schrödinger equation $i\psi_t(z, t) = -\psi_{zz}(z, t) + V(z)\psi(z, t)$. The continuity equation is $\rho_t(z, t) + j_z(z, t) = 0$, where the local probability density and current are

$$\rho(z, t) \equiv \psi^*(-z, t)\psi(z, t), \quad (1)$$

$$j(z, t) \equiv i\psi_z^*(-z, t)\psi(z, t) - i\psi^*(-z, t)\psi_z(z, t). \quad (2)$$

In this paper we limit our discussion to wave functions ψ that are eigenstates of H ; for such states the density $\rho(z)$ is time independent and the current $j(z, t)$ vanishes. The density $\rho(z)$ is *not* the absolute square of $\psi(z, t)$ and it is *analytic* in the complex- z plane.

A locally conserved probability density must be real and positive and its spatial integral must be normalized to unity. While $\rho(z)$ satisfies a continuity equation, it cannot be a probability density because it is complex-valued. We propose a novel approach. We construct a complex contour C satisfying three conditions:

$$\text{Condition I : } \quad \text{Im}[\rho(z) dz] = 0, \quad (3)$$

$$\text{Condition II : } \quad \text{Re}[\rho(z) dz] > 0, \quad (4)$$

$$\text{Condition III : } \quad \int_C \text{Re}[\rho(z) dz] = 1. \quad (5)$$

For brevity, we discuss the harmonic-oscillator ground state $\psi_0(z) = e^{-z^2/2}$ for which $\rho(z) = e^{-x^2+y^2-2ixy}$. Since $dz = dx + idy$, Condition I gives

$$dy/dx = \sin(2xy)/\cos(2xy), \quad (6)$$

which is a differential equation for the contour C . On the contour defined by this differential equation the local contribution $\rho(z) dz$ to the probability is real.

Next, we turn to Condition III. Inserting (6) into (5), we get two forms for the probability integral:

$$I = \int_C dx \frac{e^{[y(x)]^2 - x^2}}{\cos[2y(x)x]} = \int_C dy \frac{e^{y^2 - [x(y)]^2}}{\sin[2y(x)y]}. \quad (7)$$

These integrals converge if the contour C terminates in the two *good* Stokes' wedges of opening angle $\pi/2$ centered about the real axis, but they diverge if C terminates in the *bad* Stokes' wedges of opening angle $\pi/2$ centered about the imaginary axis.

To determine whether the contour C terminates in good Stokes' wedges we must solve (6). However, this simple-looking differential equation does not possess a closed-form solution, and we must rely on asymptotic techniques. For large x the contour C approaches the center of the good Stokes' wedge and for large y , C approaches the center of the bad Stokes' wedge:

$$y(x) \sim n\pi/(2x) \quad (x \rightarrow +\infty, n \in \mathbb{Z}), \quad (8)$$

$$x(y) \sim (m + 1/2)\pi/(2y) \quad (y \rightarrow +\infty, m \in \mathbb{Z}). \quad (9)$$

This asymptotic analysis shows that the integration paths occur in *quantized* bunches labeled by the integers m or n . Higher-order asymptotic analysis reveals that these bunches are *stable* in the bad Stokes' wedges and *unstable* in the good Stokes' wedges. This means that as $|y| \rightarrow \infty$, a path in the bad Stokes' wedge is drawn towards the quantized curves in (9), but that as $|x| \rightarrow \infty$ paths veer away from the quantized curves in (8), which we call *separatrices*. Thus, only the isolated separatrices ever reach ∞ in the good Stokes' wedges; all other curves turn around and are drawn into the bad Stokes' wedges. This remarkable behavior is illustrated in Fig. 3.

Figure 3 shows that the only continuous path connecting the two good Stokes' wedges follows the real axis. All other paths terminate in one good and one bad Stokes' wedge, and thus the probability integral (7) along such paths diverges. This instability of contours in the good Stokes' wedge in Fig. 3 is a serious and generic problem that must be overcome if we wish to extend the quantum probability density into the complex plane.

To overcome this apparently insurmountable problem, we show that if a contour satisfying (6) in the complex- z plane enters a bad Stokes' wedge along one path and then returns along a second path *in the same quantized bundle*, then the integral along the combined paths is actually convergent! This result is surprising because the integral along each path separately is exponentially divergent. To prove convergence, we examine the integral

$$I = \int_Y^\infty dy e^{y^2} \left(\frac{e^{-[u(y)]^2}}{\sin[2yu(y)]} - \frac{e^{-[v(y)]^2}}{\sin[2yv(y)]} \right), \quad (10)$$

where $u(y)$ and $v(y)$ are two solutions to (6) in the same bunch (that is, having the same value of m). The leading asymptotic behaviors of these solutions are given in (9), and in fact the entire Poincaré asymptotic expansions of $u(y)$ and $v(y)$ are identical to all orders in powers of $1/y$. However, the difference $D(y) \equiv u(y) - v(y)$ is nonzero and is exponentially small

$$D(y) \sim Ce^{-y^2} [1 + (n + 1/2)^2 \pi^2 y^{-2}/4 + \dots] \quad (11)$$

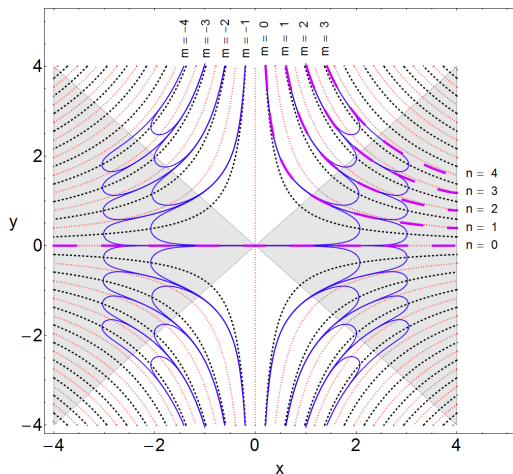


FIG. 3: Numerical solutions (solid curves) to the differential equation (6) in the complex- $z = x + iy$ plane. Solutions have vanishing slope on lightly dotted hyperbolas and infinite slope on heavily dotted hyperbolas. In the *good Stokes' wedges* (dark shading) $\rho(z)$ decays exponentially and in the *bad Stokes' wedges* (unshaded) $\rho(z)$ grows exponentially. The only curves that reach $\pm\infty$ in the good wedges are separatrices (heavy dashed curves labeled $n = 0, \dots, 4$). A typical solution curve in a good Stokes' wedge is unstable; as $x \rightarrow \infty$ the curve turns away from the separatrix, leaves the wedge, and is drawn into a bad Stokes' wedge. In the bad wedge curves are stable and continue on to $\pm i\infty$ in quantized bunches labeled by m . The only continuous unbroken curve connecting the two good wedges is the special separatrix on the real axis.

as $|y| \rightarrow \infty$, where C is an arbitrary constant. This result reflects the *hyperasymptotic* (asymptotics beyond all orders) content of (6) [19].

Using (11), we approximate the integral (10):

$$I \sim C(-1)^n(n + 1/2) \int_Y^\infty dy y^{-3} \quad (Y \rightarrow \infty), \quad (12)$$

which is convergent. Thus, while there is no continuous path running between the two good Stokes' wedges, there do exist paths connecting these wedges that repeatedly enter and re-emerge from bad Stokes' wedges. On these contours the probability integral I in (7) exists. Several such paths are shown in Fig. 4.

Figure 5 is a generalization of Fig. 4 for the first excited state of the quantum harmonic oscillator. Note that contours that connect the two good Stokes' wedges may or may not pass through the node at the origin.

We do not present the argument in this paper, but along the contours shown in Figs. 4 and 5 Condition II in (4) is satisfied. That is, along the entire complex contour obeying the differential equation (6) the local contribution to the total probability integral is positive. Thus, the requirements in the three conditions (3 – 5) are met, and we have successfully extended the probabilistic interpretation of quantum mechanics into the complex plane.

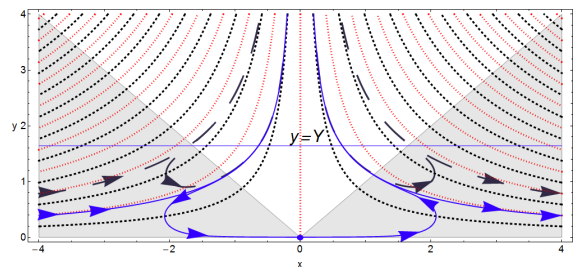


FIG. 4: Complex contours connecting good Stokes' wedges. A contour (solid curve) begins at $x = -\infty$ in the left good Stokes' wedge (shaded), leaves the wedge along a separatrix, and runs up to $i\infty$ in the bad Stokes' wedge (unshaded). The contour continues downward along a path in the same bunch, crosses the imaginary axis at $y = 0.003\,324\,973\,872\,707\,912$, and heads upwards into the same bad Stokes' wedge. Finally, the contour re-emerges from the bad Stokes' wedge and continues towards $x = +\infty$ along a separatrix in the right good Stokes' wedge. Contours have zero slope on lightly dotted lines and infinite slope on heavily dotted lines. A second contour (dashed curve) connecting the two good Stokes' wedges visits the bad Stokes' wedge four times instead of twice.

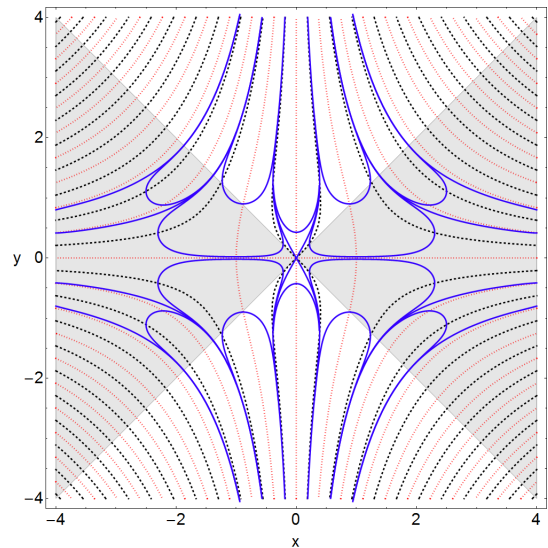


FIG. 5: Complex contours for the first excited state of the quantum harmonic oscillator. Four contours (solid lines) that begin at $x = -\infty$ in the left good Stokes' wedge (shaded) are shown. These contours leave this wedge along separatrices and run off to $\pm i\infty$ in the upper and lower bad Stokes' wedges (unshaded). After visiting a bad Stokes' wedge several times, the contours may pass through the node at the origin at 60° angles to the horizontal. At this node the probability density vanishes. Then the contours repeat the process in the right-half plane and eventually enter the right good Stokes' wedge along separatrices. It is also possible to have a complex contour that avoids the node at the origin and still connects the good Stokes' wedges. Solution curves are horizontal on lightly dotted lines and vertical on heavily dotted lines.

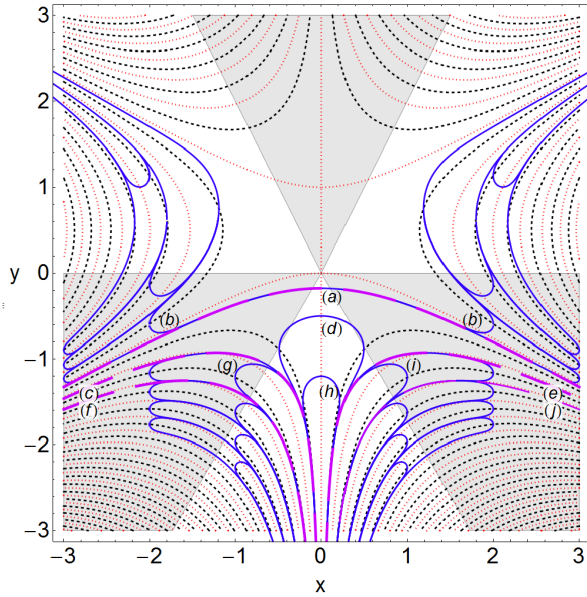


FIG. 6: Complex contours (heavy dashed lines) for the ground state ($J = 1$) of the quasi-exactly-solvable \mathcal{PT} anharmonic oscillator. A separatrix (a) goes directly from the left good Stokes' wedge to the right good Stokes' wedge, crossing the imaginary axis at $y = -0.176\,651\,795\,619\,462\,368$. Paths (b) that cross the imaginary axis at higher points than the (a) path cannot reach ∞ in the good wedge. Because they are unstable, such paths turn around, enter the upper bad Stokes' wedges, and can never re-emerge. A separatrix (c) leaves the left good wedge. This path enters the lower bad wedge to the left of the imaginary axis, re-emerges along paths (d) or (h), and reenters the bad wedge to the right of the imaginary axis. It then continues into the right good wedge along the separatrix (e). Another separatrix (f) leaves the left good Stokes' wedge, enters the lower bad Stokes' wedge, leaves and returns along (g), leaves, reenters again along (d) or (h), leaves and reenters along (j), and finally enters the right good wedge along the separatrix (f). Solution paths are horizontal on lightly dotted lines and vertical on heavily dotted lines.

The analysis in this paper is general and extends to other \mathcal{PT} quantum theories, such as the quasi-exactly solvable quartic anharmonic oscillator, whose Hamiltonian is $H = p^2 - x^4 + 2ix^3 + x^2 + 2iJx$ [20]. However, for quantum theories other than the harmonic oscillator, there are two kinds of bad Stokes' wedges: (1) wedges for which there exist probability contours C that enter and re-emerge from the wedge and for which the probability integral along C converges and (2) wedges for which no such contour exists. For the Hamiltonian above there are three good Stokes' wedges and three bad Stokes' wedges, one of type (1) and two of type (2) (see Fig. 6).

The quantum probability densities associated with the curves in Figs. 4, 5, and 6 resemble pup tents with ripples in their canopies, in contrast to the smooth surface in the classical pup tent in Fig. 2. This is the complex analog of Fig. 1 and illustrates the complex correspon-

dence principle.

CMB thanks the U.S. Department of Energy and DWH thanks Symplectic Ltd. for financial support.

* Electronic address: cmb@wustl.edu

† Electronic address: d.hook@imperial.ac.uk

‡ Electronic address: pnm@physics.wustl.edu

§ Electronic address: phywq@nus.edu.sg

- [1] C. M. Bender, S. Boettcher, and P. N. Meisinger, *J. Math. Phys.* **40**, 2201 (1999).
- [2] F. Calogero *et al.*, *J. Phys. A: Math. Gen.* **38**, 8873-8896 (2005); Yu. Fedorov and D. Gomez-Ullate, *Physica D* **227**, 120 (2007).
- [3] C. M. Bender, J.-H. Chen, D. W. Darg, and K. A. Milton, *J. Phys. A: Math. Gen.* **39**, 4219 (2006); C. M. Bender and D. W. Darg, *J. Math. Phys.* **48**, 042703 (2007).
- [4] C. M. Bender, D. D. Holm, and D. W. Hook, *J. Phys. A: Math. Theor.* **40**, F81 (2007); *ibid.* F793-F804 (2007).
- [5] A. Fring, *J. Phys. A: Math. Theor.* **40**, 4215 (2007).
- [6] A. V. Smilga, *J. Phys. A: Math. Theor.* **42**, 095301 (2009).
- [7] C. M. Bender *et al.*, *Pramana J. Phys.* **73**, 453 (2009).
- [8] In the physical world the classically forbidden region is accessible. For example, in optics when the angle of incidence at an interface is less than a critical angle, there is no transmitted wave. The electromagnetic field crosses the boundary but is attenuated exponentially beyond the interface. This field does not vanish in the classically forbidden region, but there is no flux of energy; that is, the Poynting vector vanishes in the classically forbidden region. In complex classical mechanics particles enter the classically forbidden region but there is no particle flow parallel to the real axis; the flow of particles is *orthogonal* to the axis. This feature is analogous to the vanishing flux of energy in the case of total internal reflection. See J. D. Jackson, *Classical Electrodynamics* (John Wiley & Sons, Hoboken, 1999), Third Ed., Secs. 7.4 and 8.1.
- [9] C. M. Bender, D. C. Brody, and D. W. Hook, *J. Phys. A: Math. Theor.* **41**, 352003 (2008).
- [10] C. M. Bender and S. Boettcher, *Phys. Rev. Lett.* **80**, 5243 (1998).
- [11] P. Dorey, C. Dunning, and R. Tateo, *J. Phys. A: Math. Gen.* **34** L391 (2001); *ibid.* **34**, 5679 (2001).
- [12] A. Mostafazadeh, *J. Math. Phys.* **43**, 205 (2002) and *ibid.* 2814 (2002).
- [13] C. M. Bender, D. Brody and H. F. Jones, *Phys. Rev. Lett.* **89**, 270401 (2002); *ibid.* **92**, 119902E (2004).
- [14] C. M. Bender, *Contemp. Phys.* **46**, 277 (2005) and *Repts. Prog. Phys.* **70**, 947 (2007).
- [15] P. Dorey, C. Dunning, and R. Tateo, *J. Phys. A: Math. Gen.* **40**, R205 (2007).
- [16] Z. H. Musslimani *et al.*, *Phys. Rev. Lett.* **100**, 030402 (2008).
- [17] K. G. Makris *et al.*, *Phys. Rev. Lett.* **100**, 103904 (2008).
- [18] A. Guo *et al.*, *Phys. Rev. Lett.* **103**, 093902 (2009).
- [19] M. V. Berry and C. J. Howls, *Proc. Roy. Soc. A* **430**, 653 (1990); M. V. Berry in *Asymptotics Beyond All Orders*, ed. by H. Segur, S. Tanveer, and H. Levine (Plenum, New York, 1991), pp. 1-14.
- [20] C. M. Bender and S. Boettcher, *J. Phys. A: Math.*

Gen. **31**, L273 (1998)